Check for
updates

Design of Fractional-Order Chebyshev Low-Pass Filter for Optimized Magnitude Response Using Metaheuristic Evolutionary Algorithms

Ritu Daryani[1] · Bhawna Aggarwal[1] · Maneesha Gupta[1]

Abstract
The research work presented in this paper discusses the traditional methods of design of fractional-order filters and their shortcomings and proposes a method of deriving the physically realizable Chebyshev low-pass fractional-order filters of order $(1 + \alpha)$ which produce an optimum magnitude response. The filters of $(1 + \alpha)$ order are derived in terms of a rational transfer function of order $N = 3$. The proposed method utilizes different nature-inspired evolutionary metaheuristic algorithms which traverse the non-uniform, multidimensional, multimodal, nonlinear space and produce the coefficients of the polynomial for desired filters effectively. Comparisons are made between the reported literature and presented work on various key factors like robustness and magnitude errors in stopband and passband. It has been observed that the proposed work outperforms the work reported in the literature with minimum and maximum errors being $-58.9\,\text{dB}$ and $-31.46\,\text{dB}$. SPICE implementations of the proposed filters by operational amplifiers (Op-Amps) and operational transconductance amplifiers (OTAs) have been shown. It is observed that the implemented filters closely follow the magnitude curve of ideal filters with a mean square errors of $-74.97\,\text{dB}$ and $-70.94\,\text{dB}$ for 1.5-order and $-69.81\,\text{dB}$ and $-86.13\,\text{dB}$ for 1.7-order filters for Op-Amp and OTA-based filters, respectively. This justifies the feasibility and accuracy of the proposed filters in practical environment.

✉ Ritu Daryani
ritu.ec19@nsut.ac.in

✉ Bhawna Aggarwal
kbhawnagarg@yahoo.co.in

Maneesha Gupta
maneeshapub@gmail.com

[1] Electronics and Communication Engineering Department, Netaji Subhas University of Technology, New Delhi 110078, India

Ⓑ Birkhäuser

1 Introduction

Fractional calculus is a branch of mathematics related to the differentiation and integration of orders that are non-integer in nature. The branch has gained popularity in various fields and is being used in multiple interdisciplinary and applied fields [20] including bio-instrumentation [46, 58], control systems [11, 21], signal processing [6, 7, 56], circuits [51, 54, 61], and agriculture and modelling [33, 39, 63]. The fractional-order circuits offer the advantage of having greater degrees of freedom based on their parameters as compared to the integer order [60]. They also offer the advantage of exploiting the intermediate range of attenuation which helps to process the dynamic nature of real-world applications. A lot of research works have been followed to realize the fractional elements physically [5, 10, 13, 19, 40]. Though there are FOEs present as supercapacitors, electrolytic capacitor, etc. [47], the open literature related to circuit-based realizations suggests that compact integrated circuits for FOE are still unavailable. Therefore, various approximation techniques like continued fraction expansion (CFE) and rational approximation (RA) [49] are used for the realization of fractional circuits from integer-order circuits using passive RC tree networks [69]. The general fractance device or the constant phase element (CPE) has been used to realize different electrical and electronic circuits, especially the fractional-order filters (FOFs) and their analogue counterpart [4, 27, 53]. These analogue circuits can be designed using basic building blocks such as operational amplifiers (Op-Amps), current conveyers (CCs), and operational transconductance amplifiers (OTAs).

The fractional-order calculus is based on two general approaches of defining the derivatives of fractional orders: (1) Riemann–Liouville (RL) and (2) Caputo [49]. These techniques define the αth-order differentiation and integration of a function. Realization of these techniques is based on fractional-order elements. In the circuit theory, a fractional-order element is defined as an element with impedance Z(s) proportional to s^{α}, where α is the fractional order and κ is a constant [30, 36] and is defined as

$$Z(s) = \kappa s^{\alpha} \tag{1}$$

One of the most common applications of fractional-order arithmetic in electrical and electronic circuits to design FOFs which explore the intermediate range of attenuation and are used in signal processing. The filters are designed utilizing either fractional-order elements [30] or their equivalent ladder network defined by mathematical approximations like CFE and RA [12, 66].

Chebyshev filters are one such filters that find applications in signal processing and biomedical instrumentation. They are popular for separating different groups of frequencies and are widely used in the filtering of biomedical signals like ECG [14, 32, 57] and speech signal processing. Chebyshev filters offer higher speed and faster roll-off [61] compared to other filters. The faster roll-off is attained by allowing ripples in either passband or stopband. These filters derive their name from Chebyshev
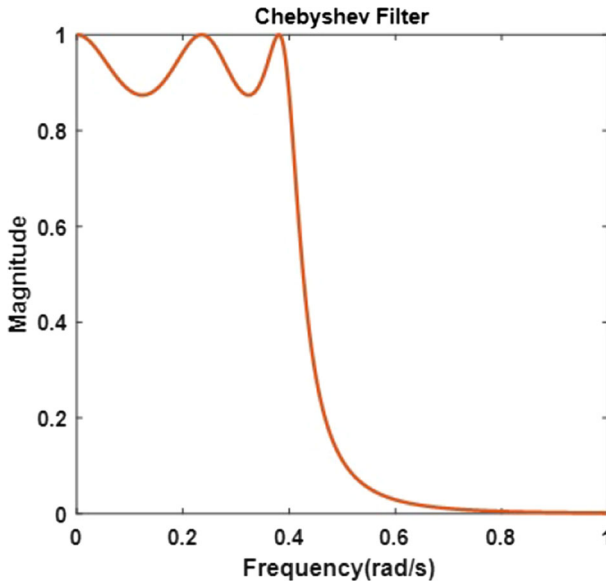
Fig. 1 Magnitude response of Chebyshev low-pass filter

polynomials given by P.L. Chebyshev. The polynomial defines the filter characteristics and is used as a design parameter. The filters are distinguished as type 1 and type 2 filters depending on if the ripples exist in the passband or stopband, respectively. The proposed work deals with the design of a fractional-order type 1 Chebyshev filter. The magnitude response for a normalized type 1 Chebyshev filter [61] is defined as

$$|H_n(j\omega)|^2 = \frac{1}{1 + \epsilon^2 C_n^2(\omega)} \tag{2}$$

where C_n is Chebyshev polynomial of order n dependent on the frequency ω (rad/s) and ϵ is defined in terms of prescribed passband attenuation as $\epsilon = \sqrt{10^{\alpha_{max}/10} - 1}$. α_{max} is the maximum attenuation of passband and is considered as 3 dB in this work, producing the value of $\epsilon = 0.996$. The magnitude response of type 1 Chebyshev filter given by (2) is presented in Fig. 1.

The design of Chebyshev filters can be extended in the fractional domain as well. Most of the fractional-order Chebyshev filters design methods reported in the literature depend upon approximating the desired fractional-order filters with next higher integer-order filter. This design methodology fails to produce an optimum magnitude response as compared to the ideal Chebyshev filter response. The motivation behind this work is to design a simple, reliable, and efficient fractional-order low-pass Chebyshev filter (FOLCF) such that the magnitude response obtained closely approximates the behaviour of an ideal FOLCF. The proposed method uses nonlinear optimization to compare a continuous-time rational polynomial with the magnitude response of the desired filter over a multidimensional, multimodal, non-uniform search space. In this method, the ideal magnitude response of a type 1 Chebyshev filter of fractional-order

has been approximated as a transfer function of integer order. The optimization is performed by using metaheuristic evolutionary algorithms [45]. Section 2 discusses the fractional-order filters and the literature related to the design and applications. The proposed design and methodology are introduced in Sect. 3 along with the design equations. Different metaheuristic algorithms utilized to design the filter are discussed as well. In the Results section, the optimized filters are presented as a graphical comparison between the magnitude of the integer-order filters and derived fractional-order filters. Further, in this section, the results obtained from different metaheuristic optimization algorithms such as particle swarm optimization, firefly algorithm, and real genetic algorithm are compared based on the errors of stopband and passband and the computation time involved. The obtained filters are also compared with different designs available in the literature to display the superiority of the proposed design. The higher-order FOLCF designs are proposed and compared with the existing literature. The SPICE implementation of the optimized filter is carried out using operational amplifiers and operational transconductance amplifier (OTA), and a comparison of the transfer characteristics of the realized filter with the ideal filters has been made in the Simulation section followed by the conclusion of the work.

2 Fractional-Order Filters

Fractional-order filters offer a great advantage over integer-order filters and are widely used for signal processing, control systems, biomedical instrumentation, etc. [8, 9, 22, 29, 34, 42, 62, 65]. These filters offer the possibility of continuous variation in the rate of attenuation in the transition band. Therefore, extensive research is being done in the field of fractional-order filter design. However, due to the unavailability of fractance elements commercially as IC components, most fractional-order filters are designed by using RC/RLC ladder networks and second-order continued fraction expansion (CFE) of s^α proposed by Freeborn et al. in [26]. The authors in [52, 55] used fractional-order capacitors to design fractional-order filters. These circuits were only stable for $(n + \alpha) < 2$ and also had issue of inherent peaking [44]. Approximation of s^α in terms of integer-order filter has been explored to design fractional-order bandpass filters [23, 44, 50].

Conventionally, the least square approximation has been used extensively to obtain equivalent counterparts of Butterworth, Chebyshev, inverse Chebyshev, and elliptical filters [2, 24, 25, 27, 37, 38, 41] in fractional domain. It helps in designing an equivalent transfer function that closely follows the response of ideal fractional-order filter by the method of curve fitting. Different techniques have been explored for the approximations of fractional-order low-pass Chebyshev filters in [23, 26, 42, 44, 52, 53, 55]. In [2], a fractional-order complex Chebyshev filter has been designed by exploring the fractional-order differentiation of the Chebyshev polynomial. The polynomial is solved using fractional Taylor series. The obtained solutions are realized using CFOA, and the Valsa CPE technique is used to approximate the fractional-order elements. In [27] and [17], the least square method and particle swarm optimization have been used, respectively, to obtain the fractional-order filters of orders $1 + \alpha$, $2 + \alpha$ and $3 + \alpha$, where the transfer functions of the respective filters are produced by expanding the s^α

as second-order continuous fraction. The filters of orders 1.2, 1.5, and 1.8 are realized using Tow-Thomas biquad topology with LT1037 Op-Amp in [27], and the CPE is realized as a Foster- 1 ladder network using fourth-order CFE. The realization is feasible till 20kHz range due to constraints of the approximation. In [17], the filters of orders 1.2, 1.5, and 1.8 are realized by using OTA-based Tow-Thomas biquad topology. The CPE is expanded as the fifth-order CFE as Foster-1 ladder network leading to tunable FOLCF. In [64], approximation of the $1 + \alpha$ order FOLCF has been done by using different optimization algorithms like simulated annealing (SA), nonlinear search (NLS), and interior search algorithms (ISA). The filters use two CPEs of different orders for the design of desired filters. The filters are further realized using Tow-Thomas biquad topology, and both the CPEs are approximated as ladder network using fourth-order CFE. In [67], digitally programmed Chebyshev fractional-order filters of orders 1.2, 1.5, and 1.8 are designed using the nonlinear least square curve fit method. The filters are realized by using follow-the-leader topology where current mirrors are utilized as current division network. The value of s^α is expanded as second-order CFE for the design. A general method of designing FOCLF using s-plane poles has been presented in [3] where the Chebyshev polynomial is solved to design a particular filter based on the order of the filter. The realization of the CPE is done as semi-infinite ladder networks in case the $\alpha < 1$ and as general impedance converter (GIC) in case $\alpha > 1$, while in [1] filters behaving like Chebyshev low-pass filters have been designed using the integer-order poles and the effect of change of order on poles has been studied as well. The realization is done using passive filters and Sallen–Key filters. The papers [2, 17, 27, 64, 67] are designed for 3 dB ripple in the passband and use second-order CFE. A comparison of these design techniques is made in Table 1 with the proposed work. To the best of the authors' knowledge, the work done till date for designing FOLCF majorly depends on comparing second-order CFE-approximated fractional-order transfer functions with integer-order transfer functions. The second-order CFE [66] is given as

$$s^\alpha \cong \frac{(\alpha^2 + 3\alpha + 2)s^2 + (8 - 2\alpha^2)s + (\alpha^2 - 3\alpha + 2)}{(\alpha^2 - 3\alpha + 2)s^2 + (8 - 2\alpha^2)s + (\alpha^2 + 3\alpha + 2)} \tag{3}$$

This approximation methodology, however, fails to produce optimal results and leads to large mean square errors. To prove this fact, in Fig. 2 the comparisons are made between ideal responses of phase and magnitude of $s^{0.5}$ and the second-order CFE-approximated responses. The magnitude and phase responses of both are compared using MATLAB 2019b software. It is observed that approximated curve closely follows the ideal response at frequencies close to 1 rad/s. However, as the frequency range increases the responses become incongruous. This proves that the approximation method used earlier to derive the circuits lacks the precision of magnitude.

3 Proposed Work

Earlier works have majorly consisted of comparing the approximated fractional-order functions for filters with the higher integer-order transfer functions. As shown in Fig. 2,

Table 1 Comparison of the literature with the proposed work

|	Optimization algorithms used	Orders of designed filters	Comparison technique used	Approximation of s^α as CFE	Realized circuit
[27]	Nonlinear least square curve fitting	$1 + \alpha, 2 + \alpha, 3 + \alpha$	Comparison with higher integer-order second order)	Yes (fourth order)	Op-Amp-based Tow-Thomas biquad
[67]	Nonlinear least square curve fitting	$1 + \alpha$	Comparison with higher integer order	Yes (second order)	Current Mirror-based Follow-the-Leader
[17]	Particle swarm optimization	$1 + \alpha, 2 + \alpha, 3 + \alpha$	Comparison with higher integer order (second order)	Yes (fifth order)	OTA-based Tow-Thomas biquad
[64]	SA, NLS, ISA	$\alpha + \beta$	Comparison with higher integer order (second order)	Yes (fourth order)	Op-Amp-based Tow-Thomas biquad
Proposed	PSO, RGA, FA	$1 + \alpha, 2 + \alpha$	Comparison with same order	Not required	Op-Amp and OTA-based Follow-the-leader
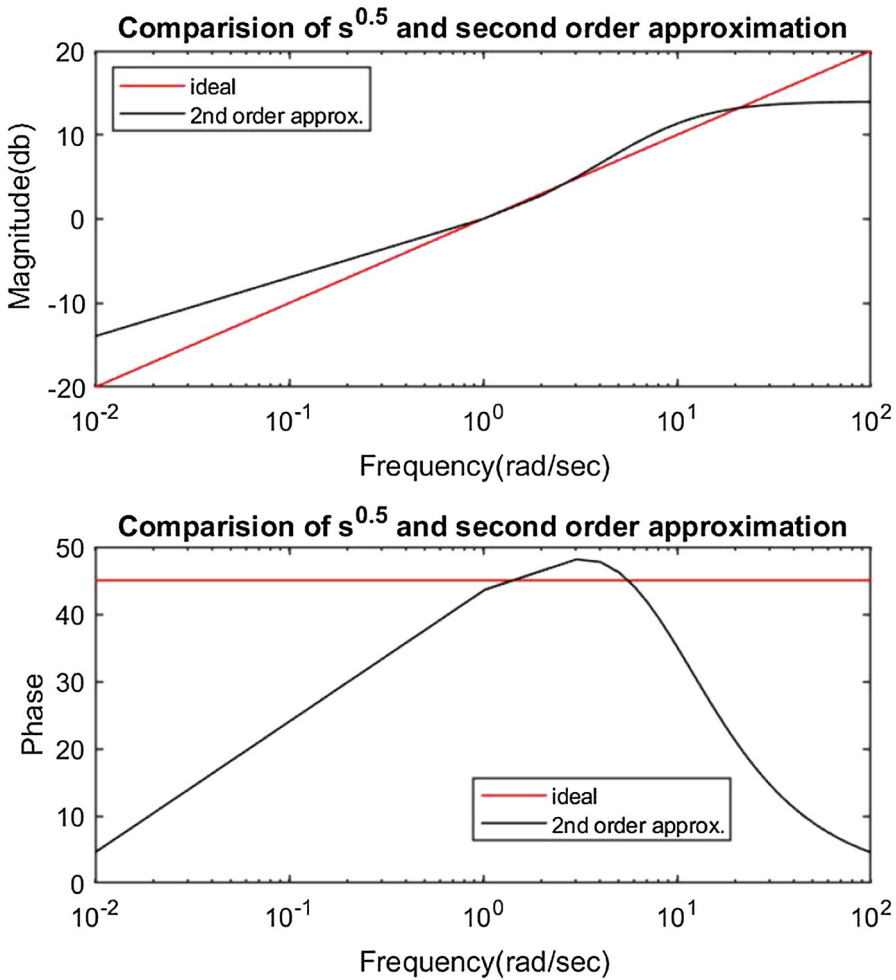
Fig. 2 Comparison of ideal and second-order continuous fractional expansion approximation of $s^{0.5}$

the error between the approximated and the ideal response of $s^{0.5}$ does not lead to optimum results. Work reported in [17, 27] used the $(1 + \alpha)$-order transfer function and compared it with the second order transfer function of the filter to obtain the values of coefficients of the desired filters. However, it has been observed that these do not produce the optimal results for magnitude response. The comparisons and approximations leave a significant error in the results. This work presents a technique that reduces this error by deriving the design equations of the rational form of $(1 + \alpha)$-order filter, by comparing its magnitude with the magnitude of the ideal $(1+\alpha)$-order filter itself. Further, it uses evolutionary algorithms to optimize the transfer function of realized FOLCF of $(1 + \alpha)$ order. In this work, three different nature-inspired evolutionary metaheuristic optimization algorithms: particle swarm optimization (PSO), firefly algorithm (FA), and real genetic algorithm (RGA) have been used for designing

the FOLCF. The designs produced by each algorithm are compared based on various key parameters like the deviation from the response of ideal $(1 + \alpha)$ fractional-order LPF, stopband and passband errors in the magnitude response. The robustness, speed, and accuracy of the algorithms have been compared further. These results predict that the transfer functions of FOLCF derived using the PSO algorithm are the most reliable, efficient, and optimal. A comparison is also drawn between the proposed work and earlier designs of FOLCF through calculations of magnitude errors. Implementation of the designed filter circuits of orders 1.5 and 1.7 based on Op-Amp 741 and OTA has been carried out using LTspiceXVII. Moreover, the magnitude responses observed are compared with the ideal filter responses.

3.1 Cost Function

The transfer function of any integer-order continuous time filter of order N can be given as a rational polynomial function of s as

$$H_I(s) = \frac{\sum_{i=0}^{M} f_i s^{M-i}}{\sum_{j=0}^{N} g_j s^{N-j}} \tag{4}$$

where $H_I(s)$ is the rational polynomial transfer function and f_i and g_j are the coefficients of the numerator and denominator polynomials, respectively, and ($i = 0, 1, 2 \ldots M$, $j = 0, 1, 2 \ldots N$). The transfer function of a normalized Chebyshev modelled low-pass filter of order n is defined by (2). The values of C_n for different integer-order filters are defined as [61]:

$$
\begin{aligned}
C_0(\omega) &= 1 \\
C_1(\omega) &= \omega \\
C_2(\omega) &= 2\omega^2 - 1 \\
C_3(\omega) &= 4\omega^3 - 3\omega \\
C_n(\omega) &= 2\omega C_{n-1}(\omega) - C_{n-2}(\omega)
\end{aligned}
\tag{5}
$$

Here, C_n is Chebyshev polynomial of order n which is also defined as a sinusoidal function given as

$$
\begin{aligned}
C_n(\omega) &= \cos(n \cos^{-1} \omega) && ; \omega < 1 \\
C_n(\omega) &= \cosh(n \cosh^{-1} \omega) && ; \omega \geq 1
\end{aligned}
\tag{6}
$$

For $\omega \geq 1$, cosh is used in place of cos, else the value of C_n in (6) will be undefined for $\omega > 1$. The series expansion of (6) produces the defined values of C_n for integer-order filters as shown in (5). To obtain the transfer characteristic of a $(n + \alpha)$-order FOLCF, (6) can be transformed and Chebyshev polynomial $C_{n+\alpha}$ can be given as [31]:

$$C_{n+\alpha}(\omega) = \cos((n + \alpha) \cos^{-1} \omega) \qquad ; \omega < 1$$

$$C_{n+\alpha}(\omega) = \cosh((n + \alpha)\cosh^{-1}\omega) \qquad ; \omega \geq 1 \qquad (7)$$

Using (2) and (7), magnitude response for a normalized FOLCF $H_C^{n+\alpha}(s)$ can be defined as

$$|H_C^{n+\alpha}(s)| = \frac{1}{\sqrt{1 + \epsilon^2 C_{n+\alpha}^2(\omega)}} \qquad (8)$$

To derive the optimal values of f_i and g_j given by (4) such that the rational polynomial function mimics the response of the fractional-order filter, the cost function for the algorithms is defined in terms of a least square error (LSE) by comparing (8) with (4) and is given as

$$\text{LSE} = \sum_{i=1}^{M} ||H_C^{n+\alpha}(\omega_i)| - |H_I(\omega_i)||^2 \qquad (9)$$

where ω(rad/s) varies from 0.01 to 10 and is sampled over $M = 10,000$ in this work. The response over this frequency range is examined to study the behaviour of both passband and stopband effectively. In this work, to design $(1 + \alpha)$-order FOLCF, a polynomial function of order $N = 3$ is chosen to match the response of fractional-order of $1 + \alpha$. The higher the order N, the more accurate the generated results are. However, it increases the complexity of the hardware circuit. Therefore, to avoid the hardware overhead and retain the accuracy of the designed filters, the orders of numerator and denominators are chosen to be $N, M = 3$. PSO along with FA and RGA is used to find the minimum value of the cost function (9). These evolutionary algorithms search through the nonlinear, multimodal, multidimensional, non-uniform search space to produce 8 coefficients $\begin{bmatrix} f_3 & f_2 & f_1 & f_0 & g_4 & g_3 & g_2 & g_1 & g_0 \end{bmatrix}$ of integer-order transfer function given by (4), which produce the minimum value of (9) and best matches the response of the Chebyshev modelled fractional-order filter.

3.2 Evolutionary Algorithms

The proposed design uses three optimization algorithms; PSO, FA, and RGA. Particle swarm optimization is one of the relatively novel metaheuristic computation techniques which is evolutionary in nature and is based on the swarm behaviour of birds and fishes [18, 35]. The equations for the algorithm are given as follows:

$$x_{i,j+1} = x_{i,j} + v_{i,j+1} \qquad (10)$$
$$v_{i,j+1} = w_j v_{i,j} + a_1 r_1 (P_{pb,i,j} - x_{i,j}) + a_2 r_2 (P_{gb,i,j} - x_{i,j}) \qquad (11)$$

where $x_{i,j+1}$ and $v_{i,j+1}$ are the position and velocity of the particle i at $j + 1$ iteration step, respectively. The PSO can be further improved by using formulations like the constriction factor method (CFM) or particle neighbourhoods [15, 35, 70, 71] which have been used in this work as

$$v_{i,j+1} = K[v_{i,j} + a_1 r_1 (P_{pb,i,j} - x_{i,j}) + a_2 r_2 (P_{gb,i,j} - x_{i,j})]$$

$$K = \frac{2}{|2 - \phi - \sqrt{\phi^2 - 4\phi}|}$$
$$\phi = a_1 + a_2; \phi > 4 \qquad (12)$$

where K is constriction coefficient depending on ϕ and ϕ depends on acceleration coefficients a_1 and a_2 as given in (12)).

The firefly algorithm is based on the flashing behaviour of the fireflies [72]. The brightness or flash of a firefly acts as an attraction agent to other fireflies. The behaviour of firefly algorithm is governed by (13) in which the attractiveness factor $\beta(r)$ decreases monotonically with respect to distance. The randomization factor κ decreases as well with each iteration to search for more precise solutions in the localized search space. The movement of each firefly x_j is calculated as a function of attractiveness and the vector between positions of two fireflies as given by (13).

$$\beta(r) = \beta_0 \exp(-\gamma r_{ij}^2)$$
$$\kappa(\text{iter}) = \frac{\kappa_{\max} - (\kappa_{\max} - \kappa_{\min})}{N} * iter$$
$$x_j = x_i + \beta_0 \exp(-\gamma r_{ij}^2) * (x_j - x_i) + \kappa * \left(\text{rand} - \frac{1}{x}\right) \qquad (13)$$

Genetic algorithms are based on techniques derived from evolution and genetics (crossovers, mutations, and selection). The versions of genetic algorithms are based on choice of mutation, crossover technique, and selection technique [28].

The pseudocodes for all three algorithms are presented in the Appendix, and the respective parameters for the algorithm are stated in Tables 2, 3, and 4. These values have been chosen by running multiple cycles of code by varying the parameters. The values of the coefficients are taken to be greater than 0.001 such that the values are positive to ensure the stability of the transfer function. Along with the necessary condition of stability, the sufficient condition has been fulfilled by including the death penalty [16] in the algorithms.

Table 2 Key parameters of PSO

Parameter	Value
$x_{\min}, x_{\max}$	0.001, 30
Population size	50
Maximum iterations	500
Velocity range	$0.2*(x_{\max} - x_{\min})$
κ	1
a_1, a_2	2.05

Table 3 Key parameters of FA

Parameter	Value
x_{min}, x_{max}	0.001, 30
Population size	50
Light absorption coefficient γ	1
Attraction coefficient β_0	2
Mutation coefficient α	0.2
Damping ratio α_{damp}	0.98
Uniform mutation range δ	$0.05 * (x_{max} - x_{min})$

Table 4 Key parameters of RGA

Parameter	Value
x_{min}, x_{max}	0.001, 30
Population size	100
P_C	1
β	1
Mutation coefficient μ	0.01
σ	0.1
Selection	Roulette wheel selection
Crossover	Double point crossover

4 Results

The cost function of the required fractional-order filter defined by (9) is optimized by running the evolutionary algorithms. These traverse the multimodal and nonlinear space to find the coefficients to produce the optimum cost by reducing the error between (4) and (8). The parameters for each algorithm are chosen specifically to obtain the best results for given number of iterations as presented in Tables 2, 3, and 4. The coefficients of the integer-order polynomial defined by (4), which is used to design the $1 + \alpha$-order filter have been obtained by running the three optimization algorithms. These coefficients are summarized in Table 5. The value of α is considered from 0.1 to 0.9. The magnitude responses of the obtained FOLCF with the specified coefficients have been plotted in linear scale in Fig. 3 and semi-log scale in Fig. 4. Plots of Figs. 3a and 4a correspond to FOLCF responses obtained through PSO, Figs. 3b and 4b correspond to FOLCF responses obtained through FA and Figs. 3c and 4c correspond to FOLCF responses obtained through RGA. In these figures, the magnitude responses for first- and second-order filters and display the behaviour corresponding to individual fractional-order by showing the required change in the slope for each curve. A slope of $-20(n + \alpha)$ dB/dec is observed corresponding to a curve associated with $(n + \alpha)$ FOF. The slopes can be seen increasing by a factor of -2 dB/dec with an increase in order by 0.1. While all three algorithms produce the filters following the ideal fractional-order Chebyshev low-pass filters, it has been observed that the plots for the PSO optimized LPFs are more accurate. This analysis has been derived from

Table 5 Values of coefficients of the rational polynomial obtained through PSO, FA, and RGA

| Optimization	f_3	f_2	f_1	f_0	g_3	g_2	g_1	g_0
$\alpha = 0.1$								
PSO	0.001	2.467	18.022	6.578	3.67	23.232	24.047	6.638
FA	0.001	0.918	14.583	14.992	1.448	18.684	29.628	14.81
RGA	0.006	13.681	9.924	10.404	16.962	23.626	21.53	10.022
$\alpha = 0.2$								
PSO	0.001	1.894	14.724	6.478	4.132	21.346	20.538	6.701
FA	0.001	2.235	19.853	10.139	5.093	28.831	29.217	10.414
RGA	0.002	12.275	10.012	10.41	18.256	23.003	22.519	9.939
$\alpha = 0.3$								
PSO	0.001	1.797	17.313	10.404	5.887	28.714	27.047	11.102
FA	0.001	1.412	17.135	13.363	4.946	29.738	30	14.171
RGA	0.016	8.84	13.174	8.63	16.816	24.946	23.445	8.6
$\alpha = 0.4$								
PSO	0.001	0.882	14.358	15.221	4.949	30	30	16.588
FA	0.001	2.891	17.804	6.461	11.136	29.805	23.984	7.331
RGA	0.047	8.675	12.5	9.554	19.188	25.633	24.457	9.795
$\alpha = 0.5$								
PSO	0.001	1.384	14.931	9.459	9.351	30	24.584	11.152
FA	0.001	1.321	14.331	9.98	8.605	29.64	24.588	11.693
RGA	0.067	8.943	10.541	8.808	20.668	23.592	22.417	9.259
$\alpha = 0.6$								
PSO	0.001	1.286	13.064	7.048	11.445	26.716	21.061	8.808
FA	0.001	0.514	12.037	11.124	8.448	30	24.321	13.649
RGA	0.033	7.463	10.023	10.807	20.47	23.739	25.663	11.48
$\alpha = 0.7$								
PSO	0.001	0.867	10.138	5.588	11.189	21.932	17.329	7.303
FA	0.001	0.355	10.199	11.089	9.092	29.625	23.383	14.268
RGA	0.038	6.712	9.014	10.297	20.582	24.155	24.251	11.659
$\alpha = 0.8$								
PSO	0.001	0.829	12.782	7.704	17.187	29.83	23.944	10.422
FA	0.001	0.724	11.324	9.145	14.187	30	23.701	12.287
RGA	0.151	5.896	10.228	9.167	22.239	25.814	24.353	11.281
$\alpha = 0.9$								
PSO	0.001	0.001	9.374	6.406	15.599	24.328	20.028	8.903
FA	0.001	1.238	16.684	4.558	29.07	29.969	27.345	6.386
RGA	0.045	3.753	10.299	7.536	21.124	24.574	22.994	9.592
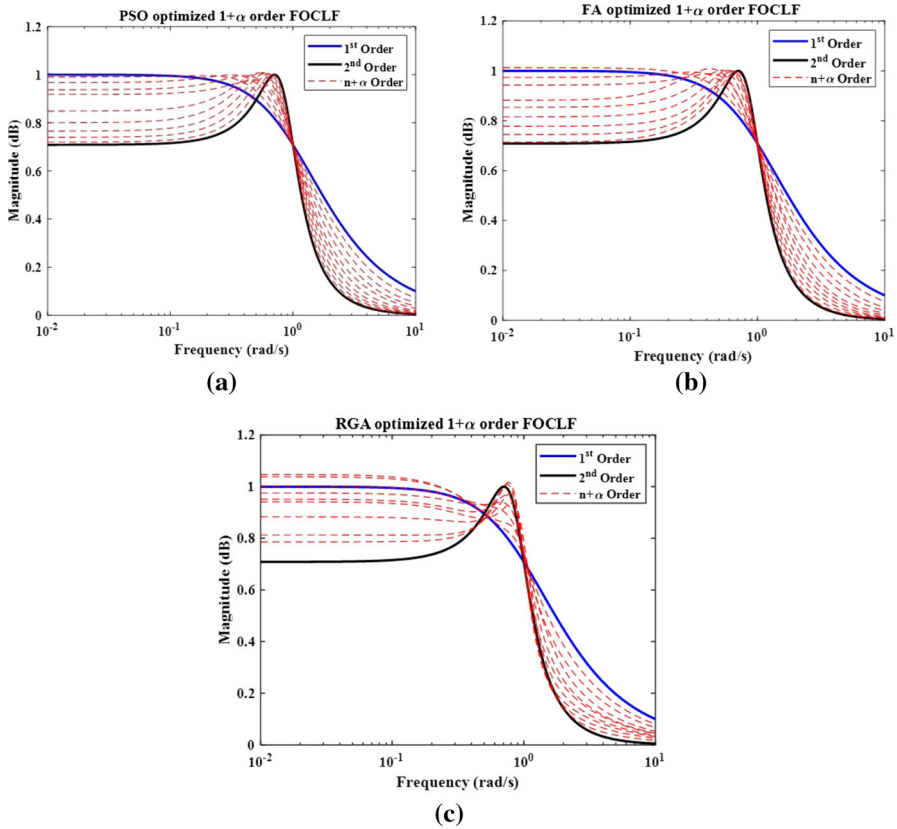
Fig. 3 Magnitude plot of $1+\alpha$-order FOLCF compared to first- and second-order Chebyshev filter in linear scale based on coefficients obtained by: **a** PSO **b** FA **c** RGA

the fact that PSO plots for fractional-order filters show properly distinguished plots, which lie within the curves of first- and second-order plots with equidistant treads. In the subsequent subsection, this observation has been confirmed analytically as well.

4.1 Comparison of Magnitude Responses of Obtained Filters

The results obtained from the three optimization algorithms are further compared on the basis of errors observed in stopband and passband. The stopband error (SE) and the passband error (PE) are calculated as [43]

$$
ERROR = 20\log_{10}\sqrt{\frac{\sum_{i=1}^{Q}||H_C^{1+\alpha}(\omega_i)| - |H_I(\omega_i)||^2}{Q}} \, \text{dB} \tag{14}
$$

where $1 < \omega < 10$ for SE and $0.01 < \omega < 1$ for PE and Q is number of frequency points over which error is measured (1000 in this work).
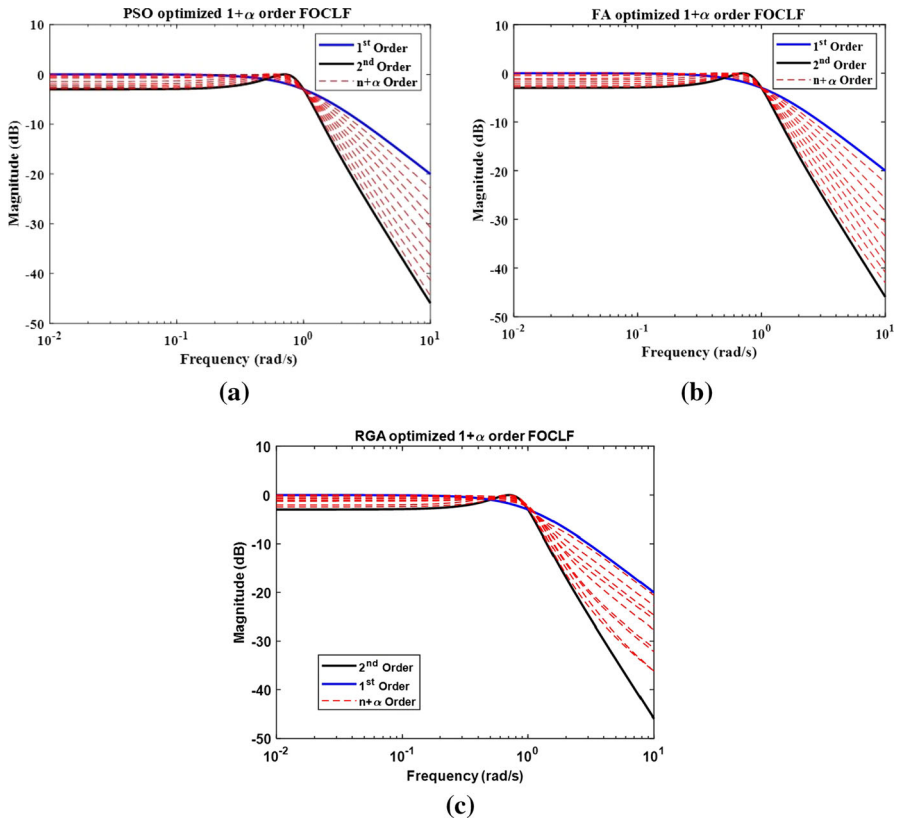
Fig. 4 Magnitude plot of $1 + \alpha$-order FOLCF compared to first- and second-order Chebyshev filter in semi-log scale based on coefficients obtained by: **a** PSO **b** FA **c** RGA

Table 6 summarizes the calculated PE and SE for all three algorithms. It is seen that the error produced by PSO in stopband and passband is minimum compared to the other two algorithms which infers that the performance of PSO obtained filters is the best among the three.

The comparative analysis of the algorithms for the passband and stopband errors is shown in Fig. 5a, b, respectively. These figures draw the error histogram for α varying from 0.1 to 0.9 for PSO, FA, and RGA. The errors for PSO are plotted as a line graph, while the errors for the FA and RGA are plotted as columns for clear comparison. The line plot for the PSO treads much below the columns of SE and PE of FA and RGA. The maximum stopband and passband errors produced by PSO are -49.86 dB and -34.99 dB for 1.6 and 1.4 order FOLCF, respectively.

4.2 Comparison of the Convergence Rate of Obtained Filters

All three algorithms are further compared on the basis of convergence and the time taken to iterate. The comparison is done by running all three algorithms for 1.5 order

Table 6 Comparison of PSO, FA, and RGA based on the values of SE and PE obtained for different orders

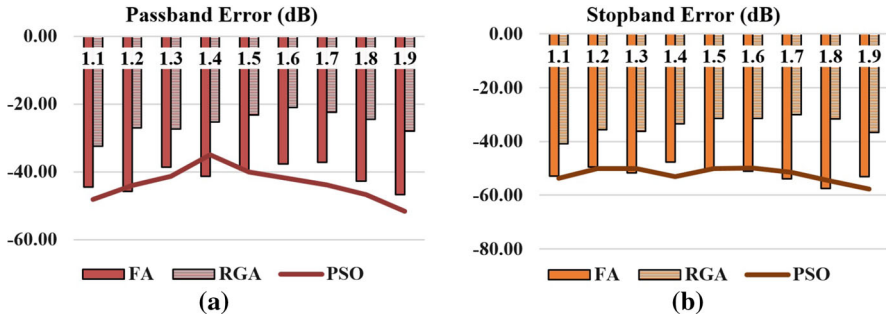|	Order	1.1	1.2	1.3	1.4	1.5	1.6	1.7	1.8	1.9
PE (dB)	PSO	−**48.08**	−44.04	−**41.36**	−34.99	−**40.1**	−**42.02**	−**43.91**	−**46.77**	−**51.6**
	FA	−44.48	−**45.72**	−38.59	−**41.4**	−39.41	−37.72	−37.15	−42.82	−46.73
	RGA	−32.43	−27.12	−27.4	−25.27	−23.31	−21.09	−22.46	−24.56	−28.05
SE (dB)	PSO	−**53.77**	−**50.1**	−50.16	−**53.17**	−50.04	−49.86	−51.44	−**54.75**	−**57.8**
	FA	−52.82	−49.5	−**51.74**	−47.64	−**50.56**	−**51.12**	−**53.88**	−57.59	−53.07
	RGA	−40.85	−35.7	−36.22	−33.43	−31.35	−31.55	−30.13	−31.72	−36.66

Fig. 5 Comparison of magnitude errors of filters obtained through PSO, FA and RGA **a** passband error **b** stopband error

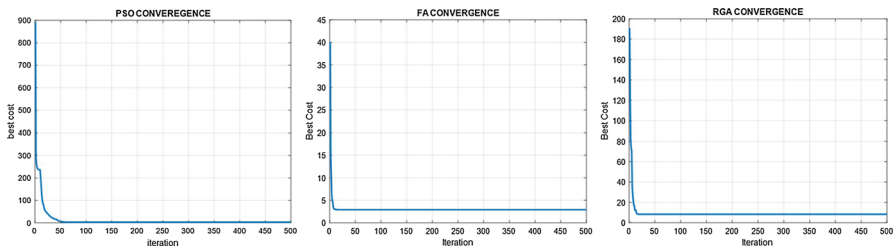**Fig. 6** Comparison of the convergence rate of three algorithms
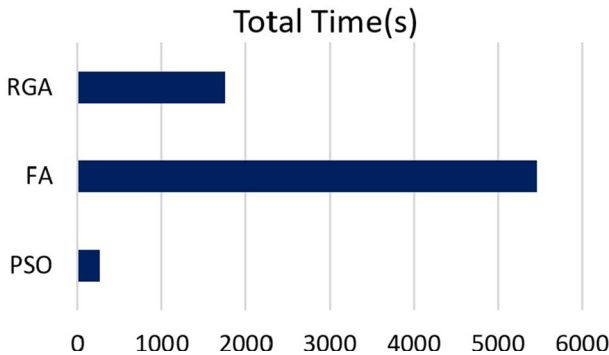

Fig. 7 Comparison of PSO, FA, and RGA based on simulation time

and recording the time of the simulation. The graphs for best cost with respect to the number of iterations are displayed in Fig. 6, and the time taken to exhaust the stopping criteria is compared in Fig. 7. The stopping criterion considered here is the number of maximum iterations. The value is taken as 500 for all three algorithms. It is observed that PSO takes the least amount of time. This is due to the fact that the PSO does not require ranking the solutions in each iteration first and then exploring the best solution, while both the real genetic algorithm and firefly algorithm require the ranking and selection of best solutions in each iteration, thus, consuming greater time.

4.3 Comparison of Magnitude Responses of Obtained Fractional-Order Chebyshev Filter Using PSO with the Literature

As discussed earlier, Chebyshev modelled low-pass fractional-order filters have been approximated and designed using different techniques in the past. Some techniques involve manipulation of the Chebyshev differential equation [2, 14]. Some involve approximating the second-order CFE of s^α for low-pass fractional-order filters with a higher integer-order Chebyshev low-pass filters [17, 27, 57, 67]. A comparison of the proposed FOLCF on the basis of stopband and passband errors for some state-of-the-art works reported in the literature on FOLCF has been made.

Table 7 along with Fig. 8a, b infers that the performance of the FOLCFs designed in present work is better as compared to the other techniques existing in the literature. It has been observed that the magnitude error generated in both the passband and the stopband is much smaller in the proposed designs. This is due to the fact that designing technique used in this paper utilizes the magnitude function of an ideal low-pass Chebyshev fractional-order filter to derive the coefficients of the continuous time rational transfer function. This helps in producing an accurate and optimum magnitude response rather than comparing the approximated fractional-order filters of $(n + \alpha)$ order with transfer function of $(n + 1)$ integer-order low-pass filter. From Table 7, it has been calculated that the stopband and passband errors observed in the proposed FOLCF are much lower than the others reported in the literature by an average of 25.98 dB.

4.4 Designing of Higher-Order Filters

The technique presented in this paper can be used to derive the higher-order FOLCFs as well. This can be done by increasing the order of denominator and numerator polynomials in (4) while ensuring the stability of the circuit. This method has been used to derive the $(2 + \alpha)$-order FOLCFs. The order of the numerator polynomial is taken as 3 $(M = 3)$ and that of the denominator polynomial is increased to 4 $(N = 4)$. The coefficients for the rational transfer function are derived using the evolutionary algorithms can be defined in terms of matrix x as

$$x = \begin{bmatrix} f_3 & f_2 & f_1 & f_0 & g_4 & g_3 & g_2 & g_1 & g_0 \end{bmatrix} \tag{15}$$

Table 8 shows the values of coefficients obtained for $(2 + \alpha)$-order Chebyshev LPF using PSO. Figure 9 shows the magnitude plot of the obtained filters, juxtaposed with the second- and third-order Chebyshev LPF. The magnitude plots of the designed $(2 + \alpha)$-order filters lie within the magnitude curves of Chebyshev low-pass filters of second and third orders and the uniform treading in the slopes over the range signifies the accurate design of the filters.

FOLCF of any desired order can be designed using the similar technique of replacing the value of C_n by $C_{(n+\alpha)}$ where $(n + \alpha)$ corresponds to the order of the desired filter. The magnitude of the desired filter can be compared with the rational polynomial of

Table 7 Comparison of proposed work and state-of-the-art FOLCF reported in the literature based on the values of SE and PE obtained for different orders

	Order	1.1	1.2	1.3	1.4	1.5	1.6	1.7	1.8	1.9
PE (dB)	[17]	− 19.18	− 18.64	− 18.64	− 19.01	− 19.2	− 20.7	− 23.3	− 26.96	− 33.09
	[27]		− 13.36			− 18.49			− 26.58	
	[67]		− 15.91			− 4.39			− 9.88	
	[64]ISA	− 10.02		− 9.06	− 9.8			− 13.24		
	[64] NLS	− 7.64		− 10.15	− 12.18			− 19.78		
	[64] ISA	− 9.79		− 11.19	− 12.82			− 21.84		
	Proposed	**− 48.08**	**− 44.04**	**− 41.36**	**− 34.99**	**− 40.1**	**− 42.02**	**− 43.91**	**− 46.77**	**− 51.6**
SE (dB)	[17]	− 8.95	− 15.58	− 22.7	− 31.84	− 35.9	− 35.16	− 36.72	− 39.27	− 44.2
	[27]		− 19.66			− 39.34			− 37.87	
	[67]		− 23.8			− 25.46			− 27.02	
	[64]SA	− 24.09		− 25.51	− 29.56			− 22.57		
	[64] NLS	− 15.95		− 18.38	− 19.86			− 25.68		
	[64] ISA	− 19.37		− 21.96	− 23.36			− 38.52		
	Proposed	**− 53.77**	**− 50.1**	**− 50.16**	**− 53.17**	**− 50.04**	**− 49.86**	**− 51.44**	**− 54.75**	**− 57.8**

Values for SE and PE have been calculated only for the data of orders present in the reported literature
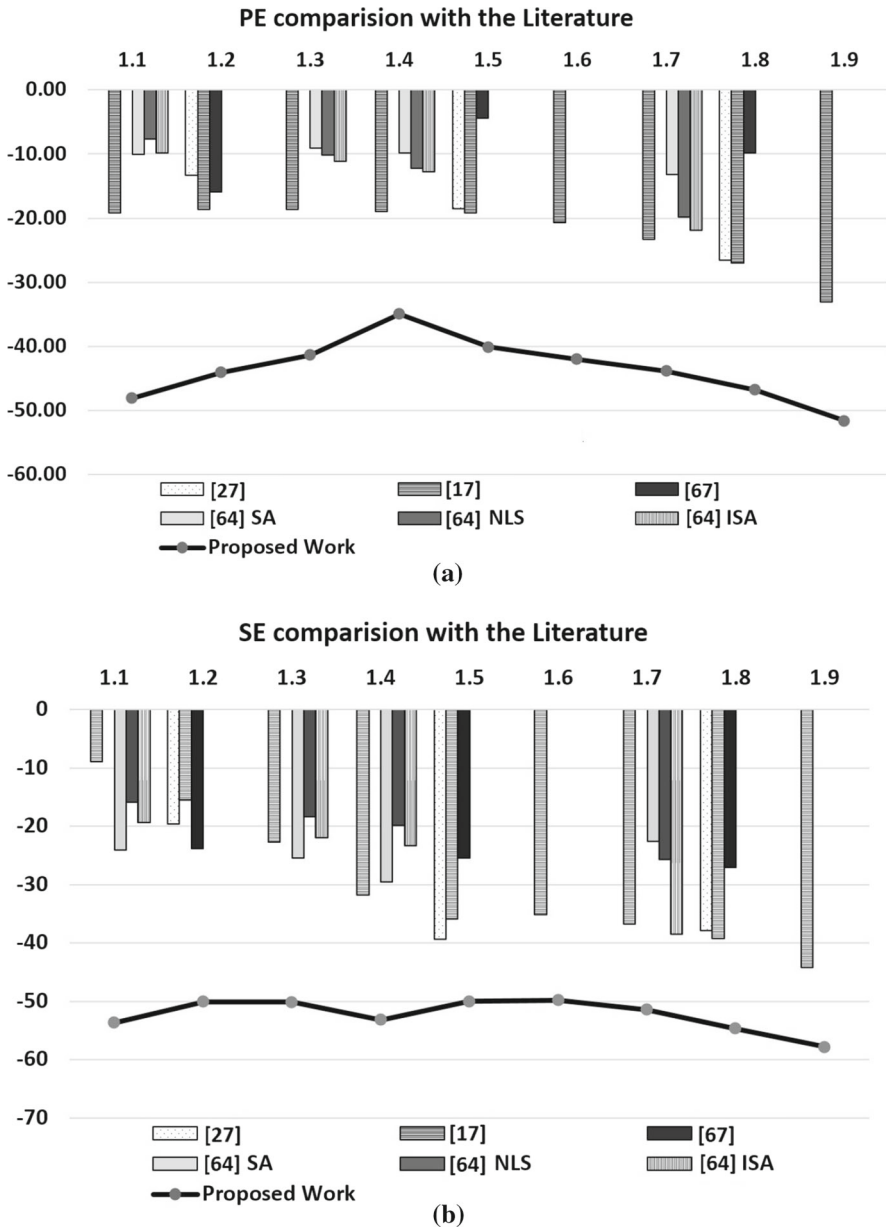
Fig. 8 Comparison of the proposed work with the reported literature based on **a** passband error and **b** stopband error

Table 8 Values of coefficients of rational polynomial obtained through PSO to design $(2+\alpha)$-order Chebyshev LPF

| Order	f_3	f_2	f_1	f_0	g_4	g_3	g_2	g_1	g_0
2.1	0.001	0.001	13.151	6.543	0.001	30	30	28.842	9.212
2.2	0.001	0.001	8.952	8.826	0.001	25.316	30	27.877	12.503
2.3	0.001	8.953	8.834	0.001	29.179	30	30	12.282	0.001
2.4	0.001	0.001	6.549	9.793	0.001	28.002	30	30	13.555
2.5	0.001	6.252	8.825	0.001	30	26.652	30	11.544	0.001
2.6	0.001	3.141	8.762	2.515	22.251	30	30	18.651	3.003
2.7	0.001	1.947	8.644	2.387	23.067	30	30	18.582	2.66
2.8	0.001	0.001	1.273	8.894	0.001	30	22.237	30	10.041
2.9	0.001	0.001	0.001	8.738	0.001	30	21.131	30	9.352
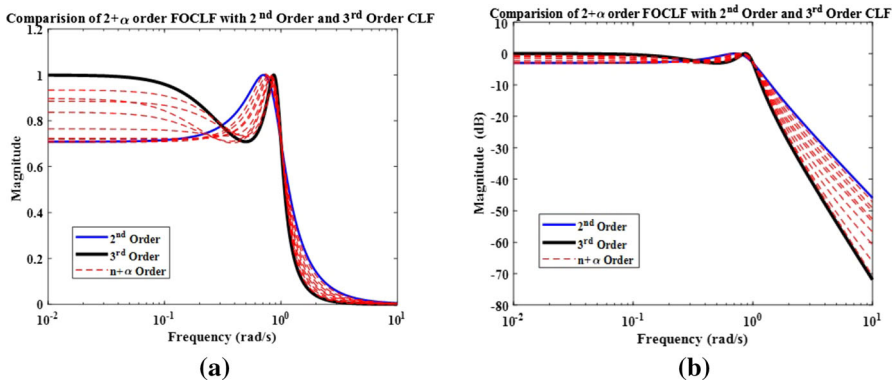
Fig. 9 Comparison of $(2 + \alpha)$-order FOLCF with the 2nd and 3rd order Chebyshev LPF **a** linear scale **b** dB scale

order N where the value of N increases with the value of n for the denominator and numerators.

4.5 Comparison of Magnitude Responses of Obtained $(2 + \alpha)$-Order Filter Using PSO with Previous Work

In this subsection, the obtained $(2 + \alpha)$-order Chebyshev filters are compared with the similar filters available in the literature. Filters of orders 2.2, 2.5, and 2.8 are compared based on stopband and passband errors in the magnitude. The comparison is made over a frequency range of $0.01 < \omega < 1$ for the passband and $1 < \omega < 10$ for the stopband. The results of the comparison are presented in Table 9. The results are further plotted graphically in Fig. 10 for a better comparison. It is observed that the SE and PE for the proposed work are much smaller than the work available in the literature. The maximum error produced in stopband is -48.84 dB for the 2.8-order

Table 9 SE and PE comparison of $(2 + \alpha)$-order FOLCF with the reported literature

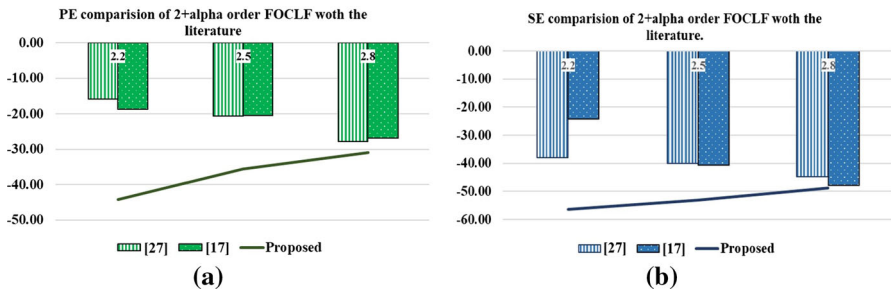|		Order	2.2	2.5	2.8
PE (dB)	PSO		**− 44.28**	**− 35.62**	**− 30.99**
	[27]		− 15.88	− 20.55	− 27.85
	[17]		− 18.71	− 20.45	− 26.9
SE (dB)	PSO		**− 56.44**	**− 53.16**	**− 48.84**
	[27]		− 38.1	− 39.98	− 44.77
	[17]		− 24.3	− 40.61	− 47.89

Fig. 10 Comparison of the proposed work with the literature based on SE and PE of magnitude for $(2+\alpha)$-order FOLCF **a** passband error **b** stopband error

FOLCF in the stopband and − 30.99 dB for 2.8 FOLCF in the passband. The errors are lower than the reported literature by an average of 14.38 dB.

4.6 Stability Analysis

The designed filters are tested on the basis of stability. During the computation stage through the algorithms, it was ensured that the obtained coefficients follow the necessary and sufficient conditions for stability. This was done by introducing a death penalty in the algorithms. Stability of the designed filters is tested by plotting the pole-zero map of the transfer functions in the s-plane. If any pole lies in the unstable region, the filter is said to be unstable. Figure 11a–c shows the pole-zero plots for $(1 + \alpha)$-order FOLCF filters obtained through PSO, FA, and RGA algorithms. Figure 11d shows the pole-zero plots for $(2 + \alpha)$-order FOLCF filters obtained through the PSO algorithm. These figures show that all the poles lie in the stable region, confirming the stability of the designed filters.

4.7 SPICE Implementation of $(n + \alpha)$-Order Filters

The rational transfer function of FOLCF can be represented as a signal flow graph shown in Fig. 12. This signal flow graph has been implemented using the Op-Amp-based follow-the-leader topology and OTA-based circuits, as shown in Figs. 13 and 14, respectively. Both circuits are realized using LTspiceXVII by implementing the trans-
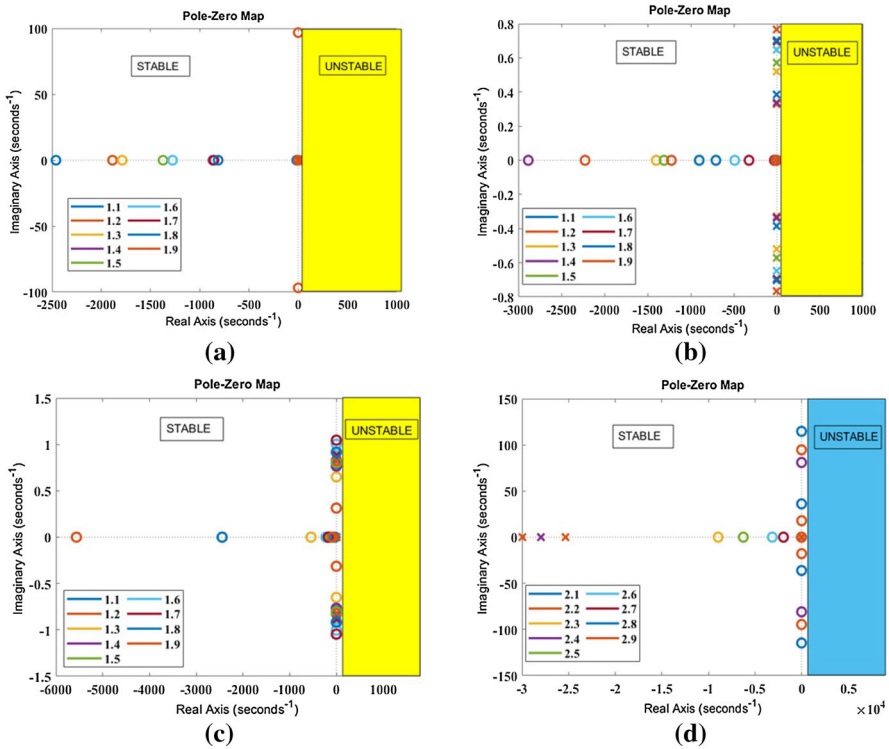
Fig. 11 Pole-zero plots for the designed filters **a** $(1 + \alpha)$ PSO **b** $(1 + \alpha)$ FA **c** $(1 + \alpha)$ RGA **a** $(2 + \alpha)$ PSO

fer function as respective circuits using Op-Amp 741 and LT1228. The time constant for the circuit is considered to be 1 ms. The values of capacitances, transconductance, and resistances have also been scaled by a factor of 1000 to ensure feasibility.

4.7.1 Design Using Op-Amp-Based Circuit

The transfer function of the SFG can be given as

$$\frac{V_{\text{out}}}{V_{\text{in}}} = \frac{b_0 s^3 + b_1 s^2 + b_2 s + b_3}{s^3 + a_1 s^2 + a_2 s + a_3}. \tag{16}$$

The feedforward and feedback path resistor values are obtained by equating the transfer function of the circuit with the canonical form of the desired fractional-order filter obtained using PSO. The circuit diagram is presented in Fig. 13, and the values of the resistors for the design of 1.5- and 1.7-order filters are presented in Table 10. All the simulations are done using LTspiceXVII. It has been observed that the slope of the 1.5-order FOLCF is -30.42 dB/dec and that of the 1.7-order filter is -34.53 dB/dec, which is very close to the ideal slopes of -30 dB/dec and -34 dB/dec for orders 1.5 and 1.7, respectively.
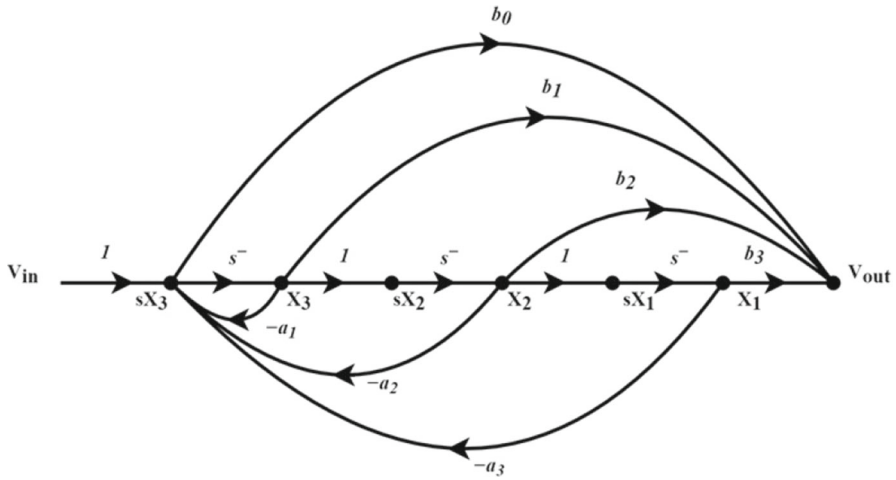
Fig. 12 Signal flow graph corresponding to the rational transfer function for $(1+\alpha)$ FOLCF implementation
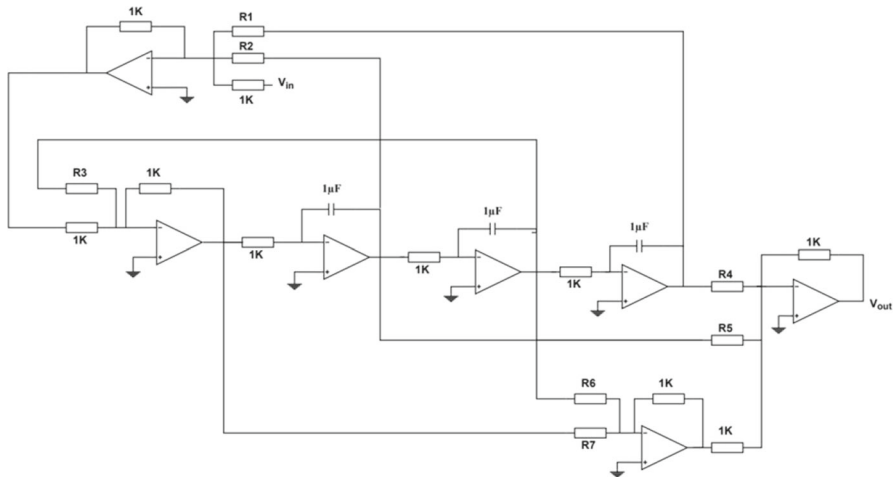
Fig. 13 Op-Amp-based equivalent circuit for design of $(1 + \alpha)$-order FOLCF

Table 10 Values of resistors for the design of 1.5- and 1.7-order FOLCF using Op-Amp-based circuit shown in Fig. 13

Resistor	1.5	1.7
$R1(\Omega)$	838.5	1.53k
$R2(\Omega)$	311.7	510.2
$R3(\Omega)$	380.4	645.7
$R4(\Omega)$	988.6	2k
$R5(\Omega)$	6.8k	12.9k
$R6(\Omega)$	626.3	1.1k
$R7(\Omega)$	9.35M	11.2M

Fig. 14 OTA-based equivalent circuit for design of $(1 + \alpha)$-order FOLCF

4.7.2 Design Using OTA-Based Circuit

The OTA-based implementation of fractional-order filters has been done in the [59, 68] as they provide compact circuits with tunability. An equivalent OTA-based circuit can be implemented based on the SFG, as shown in Fig. 14. The values of the transconductance can be found by comparing Eq. (16) with Eq. (17).

$$\frac{V_{\text{out}}}{V_{\text{in}}} = \frac{\frac{g_9}{g_4}s^3 + \frac{g_6 g_{10}}{g_4 C_1}s^2 + \frac{g_1 g_5 g_{10}}{g_4 C_1 C_2}s + \frac{g_1 g_2 g_3 g_{10}}{g_4 C_1 C_2 C_3}}{s^3 + \frac{g_7 g_{10}}{g_8 C_1}s^2 + \frac{g_1 g_{11} g_{10}}{g_8 C_1 C_2}s + \frac{g_1 g_2 g_{10} g_{12}}{g_8 C_1 C_2 C_3}} \tag{17}$$

Taking the values $g_1, g_2, g_3, g_4, g_8, C_1, C_2$ and C_3 as 1 and scaling the components by 1000 with the time constant as 1 ms, values of different circuit elements can be calculated. Table 11 shows the values obtained to design OTA-based FOLCFs of orders 1.5 and 1.7 shown in Fig. 14. The slopes obtained for the realized filters are -30.67 dB/dec and -34.46 dB/dec, respectively.

The magnitude plots produced by LTspice are shown in Fig. 15. In this figure, the frequency characteristics for the 1.5- and 1.7-order low-pass Chebyshev filter have been plotted for both Op-Amp-based circuit and OTA-based circuit. The results obtained from circuit implementation are compared with the ideal fractional-order filters. The plots showing the error curve between the magnitudes of designed filters and the ideal filters for both 1.5- and 1.7-order FOLCF are shown in Fig. 15. It can

Table 11 Values of transconductance for the design of 1.5- and 1.7-order FOLCF using OTA LT1228

Transconductance	1.5	1.7
g_5 (mS)	1.579	1.814
g_6 (mS)	0.146	0.155
g_7 (mS)	3.172	3.925
g_9 (mS)	0.107	0.089
g_{10} (mS)	1.012	0.499
g_{11} (mS)	2.599	3.101
g_{12} (mS)	1.179	1.307
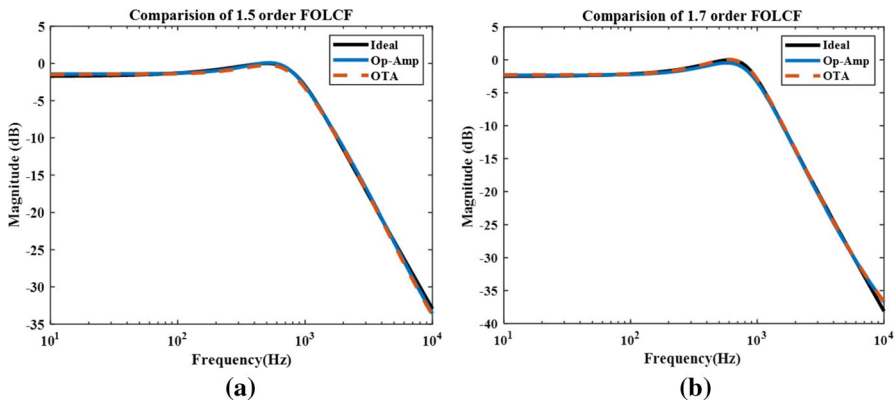
Fig. 15 Comparison of the realized filter with the ideal filter response. **a** 1.5-order FOLCF magnitude response **b** 1.7-order FOLCF magnitude response

be observed that the plots are nearly overlapping. The maximum and mean square errors between the filters are presented in Table 12. The maximum error between the curves for 1.5 order is observed to be -38.82 dB and -29.47 dB for Op-Amp and OTA, respectively, and for 1.7 order it is observed to be -24.37 dB and -44.02 dB. This is sufficient to say that the proposed design outperforms the reported literature. The improvement in the values of the magnitude errors is large, and thus the proposed design produces optimum magnitude response. Further, the realization of the filters does not involve the approximation of the CPE as ladder networks. This ensures the substantiality of the filter characteristics over a large range as opposed to approximated CPE-based filters. The comparisons of the realized 1.5- and 1.7-order filters with the ideal filter response showcase minimal error and confirm the significant feasibility of the filters. Moreover, Sect. 4.5 shows that the proposed work may be extended to design higher-order filters and the comparison with the literature of $(2 + \alpha)$-order filters showed that higher-order designs outperform the traditional designs as well.

Table 12 Error comparison of the spice implemented and the ideal 1.5- and 1.7-order FOLCF

Magnitude Error		1.5	1.7
Maximum error (dB)	Op-Amp	− 38.82	− 24.37
	OTA	− 29.47	− 44.02
Mean square error (dB)	Op-Amp	− 74.97	− 69.81
	OTA	− 70.94	− 86.13

5 Conclusion

Design of a $(n + \alpha)$-order fractional-order Chebyshev low-pass filter which gives the optimum magnitude response has been proposed in this paper. This is achieved by comparing the magnitude of the integer-order equivalent function of the desired FOLCF with the magnitude of the same ideal FOLCF. It has been observed that the stopband and passband errors produced by the design presented in this paper are much lower than designs presented in the literature with an average of 26.85 dB in the passband and 25.12 dB in the stopband. All the codes for optimization were written using MATLAB programming language and executed in MATLAB 2019b software, and SPICE implementations have been carried out using LTspiceXVII on an Intel(R) Core(TM) i7-10750H processor of 2.60 GHz, with 16 GB RAM. The optimization performed by using PSO showed the best response compared to FA and the RGA. PSO also took lesser time to exhaust the stopping criteria. This is due to the fact that PSO does not require to rank individual solutions for each iteration, unlike the FA and RGA. PSO also traverses the multimodal plane efficiently, and the chances of being trapped in the local solution are minimized. It takes into knowledge all three factors of the individual best solution, swarm best solution, and randomness. The optimized coefficients have been used to realize the canonical form of the filter. The Op-Amp-based FOLCF of orders 1.5 and 1.7 has been implemented using LTspice. The designed filters displayed the transfer characteristics of the ideal $(n + \alpha)$-order Chebyshev filter closely, and the mean and maximum errors between the proposed design and the ideal filters showed that the proposed design produces optimum magnitude response with significantly low errors. Mean square errors of − 74.97 dB and − 70.94 dB are observed for 1.5-order FOLCF designed using Op-Amps and OTAs, respectively. Similarly, for these designs the mean square errors of − 69.81 dB and − 86.13 dB are observed for 1.7-order FOLCF. The proposed work thus presents a simple, efficient, and reliable method to design $(1+\alpha)$-order fractional-order low-pass Chebyshev filters with optimum magnitude. The proposed design outperforms the reported literature effectively, and the canonical form realization proved the feasibility of the proposed design. The work can further be extended to design the higher-order filters as presented or to design the high-pass or bandpass filters in the future.

Appendix A Pseudocodes for Algorithms

PSEUDO CODE FOR PSO

begin
Randomly initialize the position **of** the population
while (number **of** iterations are < Max. Iteration)
  Evaluate fitness **of** particle swarm
  for n = 1 **to** population size
　Find personal best
　Check **for** stability **and** apply the death penalty
　Find global best
　　for x = 1 **to** dimension **of** matrix x
　　　　update position **of** particles by (12) **and** (14)
　　end for
　end for
　update the inertia weight using K
end while
end

PSEUDO CODE FOR FA

begin
Randomly initialize the position **of** the population
Compute the brightness **of** each firefly using (15a)
while (number **of** iterations are < Max. Iteration)
　for i=1 **to** n(no. **of** fireflies)
　　for j=1 **to** n
　　　if ($\beta_i < \beta_j$)
　　　　Move i towards j by (15c)
　　　end if
　　　Evaluate the brightness **of** each firefly
　　Check **for** stability **and** apply the death penalty.
　　end for
　end for
　Rank the fireflies **and** find the best solution
　end while
　end

PSEUDO CODE **FOR** RGA

begin
Randomly initialize the position **of** the population
Compute the fitness **of** each chromosome
while (number **of** iterations are < Max. Iteration)
 Select parents
 Perform Crossover
 Perform Mutation
 Generate offspring population
 for i=1 **to** n (no. **of** offspring)
  Evaluate the fitness
  Check **for** stability **and** apply the death penalty.
 end for
 Generate a **new** population **with** the best n chromosomes
end while
end

References

1. A.M. AbdelAty, A. Soltan, W.A. Ahmed, A.G. Radwan, Fractional order Chebyshev-like low-pass filters based on integer order poles. Microelectron. J. **90**, 72–81 (2019)
2. A.M. AbdelAty, A. Soltan, W.A. Ahmed, A.G. Radwan, On the analysis and design of fractional-order Chebyshev complex filter. Circuits Syst. Signal Process. **37**, 915–938 (2018)
3. A.M. AbdelAty, A. Soltan, W.A. Ahmed, A.G. Radwan, Low pass filter design based on fractional power chebyshev polynomial, in *2015 IEEE International Conference on Electronics, Circuits, and Systems (ICECS)* (2015), pp. 9–12
4. F. Abdelliche, A. Charef, R-Peak Detection Using a Complex Fractional Wavelet
5. A. Adhikary, M. Khanra, S. Sen, K. Biswas, Realization of a carbon nanotube based electrochemical fractor, in *2015 IEEE International Symposium on Circuits and Systems (ISCAS)* (2015), pp. 2329–2332
6. A. Adhikary, S. Sen, K. Biswas, Practical realization of tunable fractional order parallel resonator and fractional order filters. IEEE Trans. Circuits I Syst. Regul. Pap. **63**, 1142–1151 (2016)
7. A.S. Ali, A.G. Radwan, A.M. Soliman, Fractional order Butterworth filter: active and passive realizations. IEEE J. Emerg. Sel. Top. Circuits Syst. **3**, 346–354 (2013)
8. A.T. Azar, A.G. Radwan, S. Vaidyanathan, *Fractional Order Systems: Optimization, Control, Circuit Realizations and Applications* (Academic Press, 2018)
9. P. Bertsias, S. Kapoulea, C. Psychalinos, A.S. Elwakil, A collection of interdisciplinary applications of fractional-order circuits, in *Fractional Order Systems* (Elsevier, 2022), pp. 35–69
10. K. Biswas, S. Sen, P.K. Dutta, Realization of a constant phase element and its performance study in a differentiator circuit. IEEE Trans. Circuits Syst. II Express Briefs **53**, 802–806 (2006)
11. R. Caponetto, G. Dongola, L. Fortuna, I. Petras, Fractional order systems, in *Modeling and Control Applications*. World Scientific Series on Nonlinear Science vol. Series A (2010)
12. R. Caponetto, S. Graziani, E. Murgano, Realization of a fractional-order RLC circuit via constant phase element. Int. J. Dyn. Control **9**, 1589–1599 (2021)
13. A. Charef, Analogue realisation of fractional-order integrator, differentiator and fractional PIλDμ controller. IEE Proc. Control Theory Appl. **153**, 714–720 (2006)

14. M.S. Chavan, R.A. Agarwala, M.D. Uplane, Comparative study of Chebyshev I and Chebyshev II filter used for noise reduction in ECG signal. Int. J. Circuits Syst. Signal Process. **2**, 1–17 (2008)

15. M. Clerc, J. Kennedy, The particle swarm-explosion, stability, and convergence in a multidimensional complex space. IEEE Trans. Evol. Comput. **6**, 58–73 (2002)

16. C.A.C. Coello, Theoretical and numerical constraint-handling techniques used with evolutionary algorithms: a survey of the state of the art. Comput. Methods Appl. Mech. Eng. **191**, 1245–1287 (2002)

17. R. Daryani, B. Aggarwal, Designing of tunable fractional order Chebyshev low pass filter using particle swarm optimization. Lect. Notes Mech. Eng

18. R.C. Eberhart, Y. Shi, J. Kennedy, *Swarm Intelligence* (Elsevier, 2001)

19. A.M. Elshurafa, M.N. Almadhoun, K.N. Salama, H.N. Alshareef, Microscale electrostatic fractional capacitors using reduced graphene oxide percolated polymer composites. Appl. Phys. Lett. **102**, 232901 (2013)

20. A.S. Elwakil, Fractional-order circuits and systems: an emerging interdisciplinary research area. IEEE Circuits Syst. Mag. **10**, 40–50 (2010)

21. G. Fedele, A. Ferrise, Periodic disturbance rejection for fractional-order dynamical systems. Fract. Calc. Appl. Anal. **18**, 603–620 (2015)

22. Y. Ferdi, Fractional order calculus-based filters for biomedical signal processing, in *2011 1st Middle East Conference on Biomedical Engineering* (2011), pp. 73–76

23. T.J. Freeborn, B. Maundy, A.S. Elwakil, Field programmable analogue array implementation of fractional step filters. IET Circuits Dev. Syst. **4**, 514–524 (2010)

24. T.J. Freeborn, Comparison of $(1 + \alpha)$ fractional-order transfer functions to approximate lowpass Butterworth magnitude responses. Circuits Syst. Signal Process. **35**, 1983–2002 (2016)

25. T.J. Freeborn, A.S. Elwakil, B. Maundy, Approximated fractional-order inverse Chebyshev lowpass filters. Circuits Syst. Signal Process. **35**, 1973–1982 (2016)

26. T.J. Freeborn, B. Maundy, A. Elwakil, Towards the realization of fractional step filters, in *Proceedings of 2010 IEEE International Symposium on Circuits and Systems* (2010), pp. 1037–1040

27. T. Freeborn, B. Maundy, A.S. Elwakil, Approximated fractional order Chebyshev lowpass filters. Math. Probl. Eng. **2015**, 4–11 (2015)

28. D.E. Goldberg, *Genetic Algorithms* (Pearson Education India, 2013)

29. R.E. Gutiérrez, J.M. Rosário, Tenreiro Machado, J. Fractional order calculus: basic concepts and engineering applications. Math. Probl. Eng. **2010** (2010)

30. T.C. Haba, G.L. Loum, J.T. Zoueu, G. Ablart, Use of a component with fractional impedance in the realization of an analogical regulator of order 1/2. J. Appl. Sci. **8**, 59–67 (2008)

31. X. He, Z. Hu, Optimization design of fractional-order Chebyshev lowpass filters based on genetic algorithm. Int. J. Circuit Theory Appl. **50**, 1420–1441 (2022)

32. S.K. Jagtap, M.D. Uplane, A real time approach: Ecg noise reduction in Chebyshev type II digital filter. Int. J. Comput. Appl. **49**, 9 (2012)

33. I.S. Jesus, J.A.T. Machado, Fractional control of heat diffusion systems. Nonlinear Dyn. **54**, 263–282 (2008)

34. S. Kapoulea, C. Psychalinos, A.S. Elwakil, Fractional-order shelving filter designs for acoustic applications, in *2020 IEEE International Symposium on Circuits and Systems (ISCAS)* (2020), pp. 1–5

35. J. Kennedy, R. Eberhart, Particle swarm optimization, in *Proceedings of ICNN'95-International Conference on Neural Networks* vol. 4 (1995), pp. 1942–1948

36. M.S. Krishna et al., Fabrication of a fractional order capacitor with desired specifications: a study on process identification and characterization. IEEE Trans. Electron Dev. **58**, 4067–4073 (2011)

37. D. Kubanek, T.J. Freeborn, J.K. Dvorak, J. Dvorak, Transfer functions of fractional-order band-pass filter with arbitrary magnitude slope in stopband, in *2019 42nd International Conference on Telecommunications and Signal Processing (TSP)* (2019), pp. 655-659

38. D. Kubanek, T.J. Freeborn, J. Koton, J. Dvorak, Validation of fractional-order lowpass elliptic responses of (1+ o)-order analog filters, in *Selected Papers from the 2018 41st International Conference on Telecommunications and Signal Processing (TSP)* (2019), p. 56

39. E.K. Lenzi, M.A.F. dos Santos, M.K. Lenzi, D.S. Vieira, L.R. da Silva, Solutions for a fractional diffusion equation: anomalous diffusion and adsorption–desorption processes. J. King Saud Univ. **28**, 3–6 (2016)

40. R. Lerner, The design of a constant-angle or power-law magnitude impedance. IEEE Trans. Circuit Theory **10**, 98–107 (1963)

41. S. Mahata, S. Banerjee, R. Kar, D. Mandal, Revisiting the use of squared magnitude function for the optimal approximation of $(1+\alpha)$-order Butterworth filter. AEU Int. J. Electron. Commun. **110**, 152826 (2019)

42. S. Mahata, S.K. Saha, R. Kar, D. Mandal, Optimal design of fractional order low pass Butterworth filter with accurate magnitude response. Digit. Signal Process. **72**, 96–114 (2018)

43. S. Mahata, S.K. Saha, R. Kar, D. Mandal, Optimal design of wideband infinite impulse response fractional order digital integrators using colliding bodies optimisation algorithm. IET Signal Process. **10**, 1135–1156 (2016)

44. B. Maundy, A.S. Elwakil, T.J. Freeborn, On the practical realization of higher-order filters with fractional stepping. Signal Process. **91**, 484–491 (2011)

45. K. Michalak, Evolutionary algorithm with a directional local search for multiobjective optimization in combinatorial problems, in *Proceedings of the Genetic and Evolutionary Computation Conference Companion* (2017), pp. 7–8

46. K. Moaddy, A.G. Radwan, K.N. Salama, S. Momani, I. Hashim, The fractional-order modeling and synchronization of electrically coupled neuron systems. Comput. Math. Appl. **64**, 3329–3339 (2012)

47. A.S. Mohapatra, D.A. John, K. Biswas, A review on the realization of fractional-order devices to use as sensors and circuit elements for experimental studies and research. Fract. Order Syst. Overv. Math. Des. Appl. Eng. **8**, 9 (2022). https://doi.org/10.1016/B978-0-12-824293-3.00012-0

48. M.D. Ortigueira, J.T. Machado, The 21st century systems: an updated vision of continuous-time fractional models. IEEE Circuits Syst. Mag. **22**, 36–56 (2022)

49. I. Podlubny, I. Petráš, B.M. Vinagre, P. O'Leary, L. Dorčák, Analogue realizations of fractional-order controllers. Nonlinear Dyn. **29**, 281–296 (2002)

50. C. Psychalinos, G. Tsirimokou, A.S. Elwakil, Switched-capacitor fractional-step Butterworth filter design. Circuits Syst. Signal Process. **35**, 1377–1393 (2016)

51. A.G. Radwan, A.S. Elwakil, A.M. Soliman, Fractional-order sinusoidal oscillators: design procedure and practical examples. IEEE Trans. Circuits Syst. I Regul. Pap. **55**, 2051–2063 (2008)

52. A.G. Radwan, A.S. Elwakil, A.M. Soliman, On the generalization of second-order filters to the fractional-order domain. J. Circuits Syst. Comput. **18**, 361–386 (2009)

53. A.G. Radwan, K.N. Salama, Fractional-order RC and RL circuits. Circuits Syst. Signal Process. **31**, 1901–1915 (2012)

54. A.G. Radwan, A.M. Soliman, A.S. Elwakil, A. Sedeek, On the stability of linear systems with fractional-order elements. Chaos Solitons Fractals **40**, 2317–2328 (2009)

55. A.G. Radwan, A.M. Soliman, A.S. Elwakil, First-order filters generalized to the fractional domain. J. Circuits Syst. Comput. **17**, 55–66 (2008)

56. A.G. Radwan, Resonance and quality factor of the $RL_\alpha C_\alpha$ fractional circuit. IEEE J. Emerg. Sel. Top. Circuits Syst. **3**, 377–385 (2013)

57. N. Rastogi, Analysis of Butterworth and Chebyshev filters for ECG denoising using wavelets. IOSR J. Electron. Commun. Eng. **6**, 37–44 (2013)

58. L.M. Richard, Fractional calculus in bioengineering. Crit. Rev. Biomed. Eng. **32** (2006)

59. I.E. Sacu, M. Alci, Low-power OTA-C based tuneable fractional order filters. Electron. Comp. Mater. **48**, 135–144 (2018)

60. D. Saha, D. Mondal, S. Sen, Effect of initialization on a class of fractional order systems: experimental verification and dependence on nature of past history and system parameters. Circuits Syst. Signal Process. **32**, 1501–1522 (2013)

61. R. Schaumann, X. Mac Elwyn Van Valkenburg, H. Xiao, *Design of Analog Filters*, vol. 1 (Oxford University Press, New York, 2001)

62. Z.M. Shah, M.Y. Kathjoo, F.A. Khanday, K. Biswas, C. Psychalinos, A survey of single and multi-component fractional-order elements (FOEs) and their applications. Microelectron. J. **84**, 9–25 (2019)

63. D. Sierociuk et al., Diffusion process modeling by using fractional-order models. Appl. Math. Comput. **257**, 2–11 (2015)

64. A. Soni, M. Gupta, Performance evaluation of different order fractional Chebyshev filter using optimisation techniques. Int. J. Electron. Lett. **8**, 205–222 (2020)

65. R. Sotner, et al, Design of building blocks for fractional-order applications with single and compact active device, in *2020 43rd International Conference on Telecommunications and Signal Processing (TSP)* (2020), pp. 573–577

66. G. Tsirimokou, C. Psychalinos, A. Elwakil, *Design of CMOS Analog Integrated Fractional-Order Circuits: Applications in Medicine and Biology* (Springer, 2017)

67. G. Tsirimokou, C. Psychalinos, A.S. Elwakil, Digitally programmed fractional-order Chebyshev filters realizations using current-mirrors, in *2015 IEEE International Symposium on Circuits and Systems (ISCAS)* (2015), pp. 2337–2340
68. M.A. Valencia-Ponce et al., CMOS OTA-based filters for designing fractional-order chaotic oscillators. Fractal Fract. **5**, 122 (2021)
69. J. Valsa, J. Vlach, RC models of a constant phase element. Int. J. Circuit Theory Appl. **41**, 59–67 (2013)
70. A.I.F. Vaz, L.N. Vicente, PSwarm: a hybrid solver for linearly constrained global derivative-free optimization. Optim. Methods Softw. **24**, 669–685 (2009)
71. Y.-J. Wang, Improving particle swarm optimization performance with local search for high-dimensional function optimization. Optim. Methods Softw. Softw. **25**, 781–795 (2010)
72. X. Yang, Firefly algorithm, Lévy distributions and global optimization, in *Research and Development in Intelligent Systems* XXVI (2010)

Birkhäuser